Carmen C. Mayorga-Martinez[1]
Lenka Hlavata[1,2]
Sandrine Miserere[1]
Adaris López-Marzo[1,3]
Jan Labuda[2]
Josefina Pons[3]
Arben Merkoçi[1,4]

[1]ICN2 - Institut Catala de Nanociencia i Nanotecnologia, Campus UAB, Bellaterra, Barcelona, Spain
[2]Faculty of Chemical and Food Technology, Institute of Analytical Chemistry, Slovak University of Technology in Bratislava, Bratislava, Slovakia
[3]Departament de Química, Universitat Autònoma de Barcelona, Bellaterra, Barcelona, Spain
[4]ICREA - Institucio Catalana de Recerca i Estudis Avançats, Barcelona, Spain

Received January 31, 2013
Revised April 24, 2013
Accepted April 24, 2013

Research Article

Nanostructured $CaCO_3$-poly(ethyleneimine) microparticles for phenol sensing in fluidic microsystem

A new and simple strategy based on nanostructured $CaCO_3$-poly(ethyleneimine) (PEI) microparticles (MPs) for phenol sensing using PDMS/glass fluidic microchip is developed. This fluidic microsystem including integrated screen-printed electrodes modified with $CaCO_3$-PEI MPs and tyrosinase (Tyr) through cross-linking with glutaraldehyde, represents a low-cost platform for phenol detection. The designed fluidic microsystem improves the sensitivity of the biosensor allowing the detection of very low concentrations of phenol (up to 10 nM). This device shows high repeatability and low detection limit, is easy to be fabricated, inexpensive, disposable, and amenable to mass production.

Keywords:
Electrochemistry / Fluidic microsystem / Nanostructurated $CaCO_3$-poly(ethyleneimine) microparticles / Phenolic compounds

DOI 10.1002/elps.201300056

1 Introduction

Phenolic compounds are widely found in petrochemical products, and in wood preservatives, textiles, plastics, dyes, paper, herbicides, and pesticides [1–3]. The development of analytical methodologies for phenol quantification in various samples as well as for evaluation of their total toxicity with respect to environmental and human health is of great importance [1–5]. The amperometric tyrosinase (Tyr)-based biosensors constitute promising technology for the in situ phenol monitoring in discrete or batch systems because of a number of advantages (high selectivity, low production cost, fast response, potential for miniaturization, simple instrumentation, and easy automation) compared to classic procedures including instrumental methods (GC, LC, etc.) [1, 2, 6–8].

The combination of nanomaterials and biotechnology open a promising field for the development of the phenol biosensor. Recently, Lopez-Marzo et al. have reported new nanostructured $CaCO_3$-poly(ethyleneimine) (PEI) microparticles (MPs) with high biofunctionalizing capacity and stability (up to 8 months) with interest for biosensing [9].

On the other hand the practical application of batch systems of Tyr-based biosensors is limited by the high number of steps needed for the measurement procedure. The biosensors used in these systems have shortcomings and stability problems for the continuous batch phenol measurement. Among automated systems, flow injection analysis (FIA) has become a very versatile and efficient technique for quantitative automated analyses since its introduction 20 years ago [10]. The combination of biosensors with flow injection techniques permits the automation and integration of phenol biosensing. Additionally, this technique allows for the control of the reagent addition steps, the measurement of enzyme activity, and also simplifies the optimization of the conditions of the reaction.

In the current study, we propose the development of an amperometric $CaCO_3$-PEI/Tyr-based biosensor integrated to a flow microsystem. This phenol biosensing is achieved through a PDMS/glass fluidic platform with integrated screen-printed electrodes (SPE) modified with $CaCO_3$-PEI MPs and Tyr through cross-linking with glutaraldehyde. The automated analytical biosystems proposed can be used for online monitoring of phenol that can be of interest for future sample screening prior to the use of sophisticated measurement systems. Combining the advantages of the PDMS and

Correspondence: Professor Arben Merkoçi, ICREA, Institució Catalana de Recerca i Estudis Avançats and Nanobioelectronics & Biosensors Group, CIN2, (ICN-CSIC), Catalan Institute of Nanotechnology, Campus de la UAB, Bellaterra 08193, Barcelona, Catalonia, Spain
E-mail: arben.merkoci@icn.cat

Abbreviations: FIA, flow injection analysis; **MP**, microparticle; **PEI**, poly(ethyleneimine); **SPE**, screen-printed electrode; **Tyr**, tyrosinase

Colour Online: See the article online to view Figs. 1–4 in colour.

screen-printing technologies allows the production of reliable and low-cost microdevices. Screen-printing is a well-known technique to produce low-cost electrodes at an industrial level [11, 12].

2 Materials and methods

2.1 Materials

All chemicals reagents were purchased from Sigma-Aldrich (Spain). The inks used for the fabrication of SPE were purchased from Electroday (Twintec S.L., Badalona, Spain) and used as received. For the preparation of stock solution of 0.1 M PBS pH 6.5 and during the measurements, MilliQ water was used. The stock solution of 100 mM of phenol was prepared in 0.1 M PBS pH 6.5; 1 mg of Tyr enzyme from mushroom (≥1000 unit/mg) was dissolved in 50 μL of 0.1 M phosphate buffer at pH 6.5. One percent glutaraldehyde solution was prepared daily in MilliQ water.

2.2 Apparatus

Electrochemical measurements were performed with a model CH-Instrument potentiostat 660A electrochemical workstation from CH Instruments, Austin, TX, USA. Magnetic stirrer Lab-disc from IKA® Werke, Staufen, Germany, was used to provide the convective transport during the amperometric measurements. Two syringe pumps (standard infusion-only pump 11 Elite) from Harvard apparatus were used for injecting the phenol stock solution and buffer pH 6.5 solution, respectively. SEM analysis was performed by using an EVO (Carl Zeiss NTS, Germany).

2.3 Synthesis of $CaCO_3$-PEI MPs

Equal volumes of the PEI (4 mg/mL) containing dissolutions of $CaCl_2$ (0.33 M) in water/ethanol (1:1, v/v) and Na_2CO_3 (0.33 M) in water were quickly mixed under sonication and during 45 min at room temperature to obtain the nanostructured vaterite $CaCO_3$-PEI hybrid material. $CaCO_3$ precipitates were washed three times, air dried, collected, and saved under room temperature conditions while not in use.

2.4 Preparation of SPE and modification with $CaCO_3$-PEI and Tyr

Screen printing electrodes fabrication is based on the sequential deposition of a graphite ink, Ag/AgCl ink and insulating ink on a polyester substrate. After the deposition of each layer, a drying process is followed by keeping the polyester substrate at 120°C for 45 min (graphite) and 30 min (Ag/AgCl and insulating). A 5 μL $CaCO_3$-PEI MPS at 1 mg/mL solution drop was deposited onto the working SPE electrode surface and allowed to dry at room temperature for 20 min. A 5 μL drop of Tyr solution was deposited onto the working SPE/$CaCO_3$-PEI electrode surface and allowed to be dried at room temperature for 3 h. Finally, 5 μL of glutaraldehyde (25%) solution at 1% was dropped onto the working electrode of SPE electrode surface and let to be dried at 40°C for 30 min. The prepared SPE/$CaCO_3$-PEI/Tyr sensor was kept at 4°C while not in use.

2.5 Microdevice fabrication for phenol detection

The microchannel was based on a hybrid PDMS/glass microchip (see Fig. 1A and B). The channel was fabricated in PDMS by soft lithography [13, 14]. PDMS was poured onto an aluminum micromachined mold and cured at 65°C for 4 h. The channel was 5 mm wide, 100 μm depth, and 5 cm long. Two reservoirs were punched at the inlet and the outlet of the channel. Finally, the PDMS and glass layers were aligned and irreversibly bonded using a 30 s oxygen plasma treatment. The electrochemical detector consists of a set of three SPE. The working electrode was modified following the protocol described earlier (see Fig. 1C).

2.6 Electrochemical experiments

In order to study the characteristics of the modified electrodes surface, cyclic voltammogram measurements were carried out at the potential range of −0.55 to 0.8 V versus Ag/AgCl

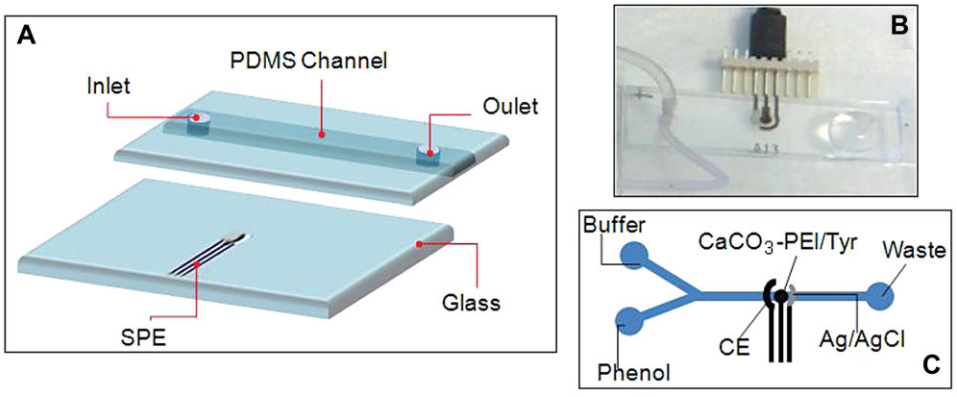

Figure 1. (A) Schematic representation of the PDMS/glass microchip device components. (B) Photograph of the PDMS/glass fluidic microsystem setup. (C) Schematic representation of the microchip design with the channel and SPE modified with $CaCO_3$-poly(ethyleneimine) (PEI) microparticles (MPs) and tyrosinase.

with 50 mv/s scan rate in 1 mM $[Fe(CN)_6]^{3-/4-}$ (1:1) as a redox indicator. Amperometric detection was performed applying −0.2 V direct current (DC) potential versus Ag/AgCl in 0.1 M phosphate buffer at pH 6.5 with 0.1 M KCl. All electrochemical experiments were carried out at room temperature.

3 Results and discussion

3.1 Characterization of the sensing surface

Figure 2 shows SEM images and cyclic voltammograms obtained from SPE (A), SPE/$CaCO_3$-PEI (B), SPE/$CaCO_3$-PEI/Tyr (C), and SPE/$CaCO_3$-PEI/Tyr/Glu (D) modified surfaces. The use of $CaCO_3$-PEI MPs represents an interesting platform for the immobilization of a large range of biomolecules, because the PEI-covered layer onto the MPs surface allows the hydrogen bond formation between the nitrogens of the amino groups in PEI and the hydrogens of the OH, NH, or SH groups present in any type of biomolecules [9]. Homogeneous distribution of the $CaCO_3$-PEI MPs onto the working electrode surface of SPE was observed (see Fig. 1B). The increase of the electron transfer through the $CaCO_3$-PEI composite was observed with the increasing of cathodic and anodic peak currents and improvement of the reversibility in corresponding cyclic voltammograms. These improvements were due to the fact that PEI is a conductive polymer [9]. The adsorption of Tyr on the $CaCO_3$-PEI cause the cathodic and anodic peak currents to decrease, indicating that Tyr has been successfully immobilized (Fig. 2C). Finally, Fig. 2D displays the effect of glutaraldehyde as a binding matrix, showing a good entrapment of the $CaCO_3$-PEI MPs and Tyr within the mentioned matrix. The cathodic and anodic peak currents decrease again when glutaraldehyde is adsorbed onto the modified SPE with $CaCO_3$-PEI and Tyr, which indicates that glutaraldehyde film was an obstacle making the electron transfer of interface more difficult. The result is consistent with that reported in literatures [15, 16].

3.2 In batch evaluation of the sensing capability of the $CaCO_3$-PEI/Tyr biosensor

The $CaCO_3$-PEI/Tyr biosensor for the phenol detection was evaluated by chronoamperometry measurement. Figure 3B depicts the chronoamperometric response for the $CaCO_3$-PEI/Tyr-based biosensor, obtained in 0.1 M PBS at pH 6.5 with 0.1 M KCl upon successive additions of 0.5 μM phenol standard solution. Current change at an increase of the phenol concentration is evident at −0.2 V DC. The observed reduction current was attributed to the direct reduction of *O*-quinone liberated from the enzyme-catalyzed reaction on the electrode surface modified with $CaCO_3$ (see Fig. 3B). For the biosensor that was not modified with $CaCO_3$ the reduction current was not observed (see Fig. 3B, red line). Tyr has hydroxylase activity, by which phenol can be hydroxylated to catechol using molecular oxygen (Eq. (1)), and also oxidase activity that can catalyze the oxidation of catechol to

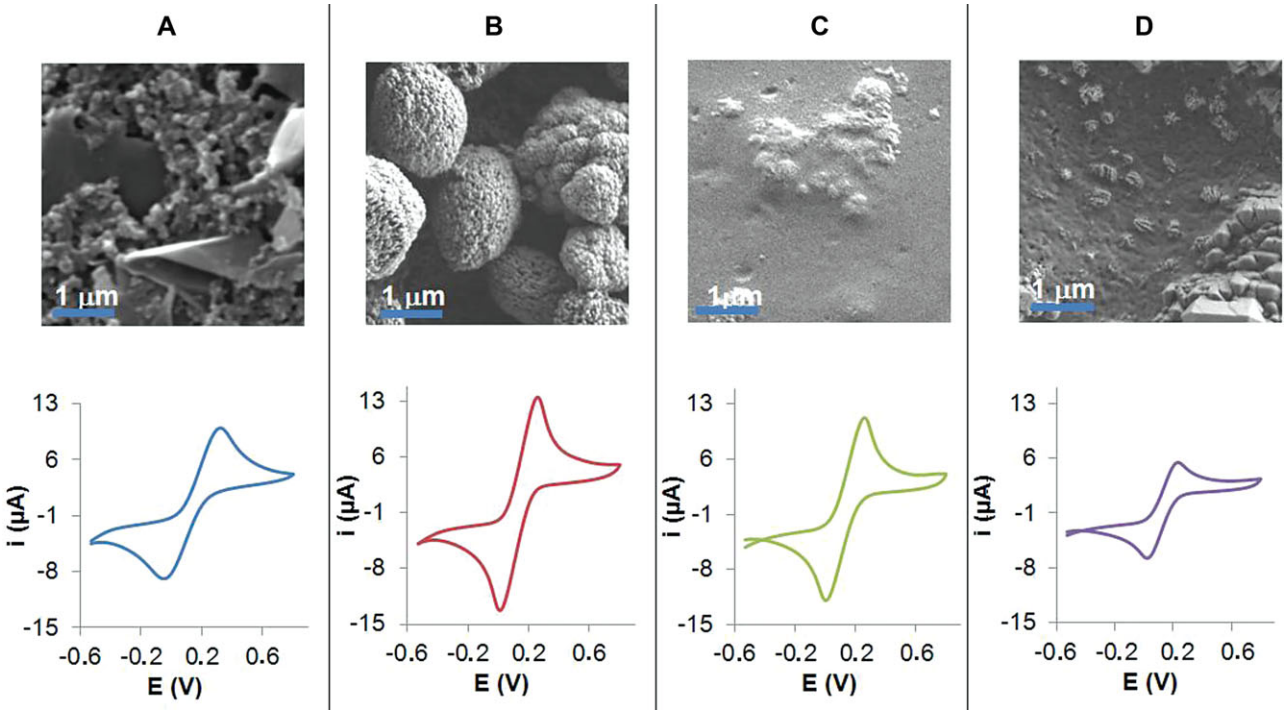

Figure 2. SEM micrographs and cyclic voltammograms of bare SPE (A) and SPE modified with: $CaCO_3$-poly(ethyleneimine) PEI MPs (B) and $CaCO_3$-PEI/tyrosinase (Tyr) (C); effect of glutaraldehyde as a binding matrix for $CaCO_3$-PEI MPs and Tyr entrapment (D). Cyclic voltammograms curves recorded at 0.05 V/s in 1 mM $[Fe(CN)_6]^{3-/4-}$.

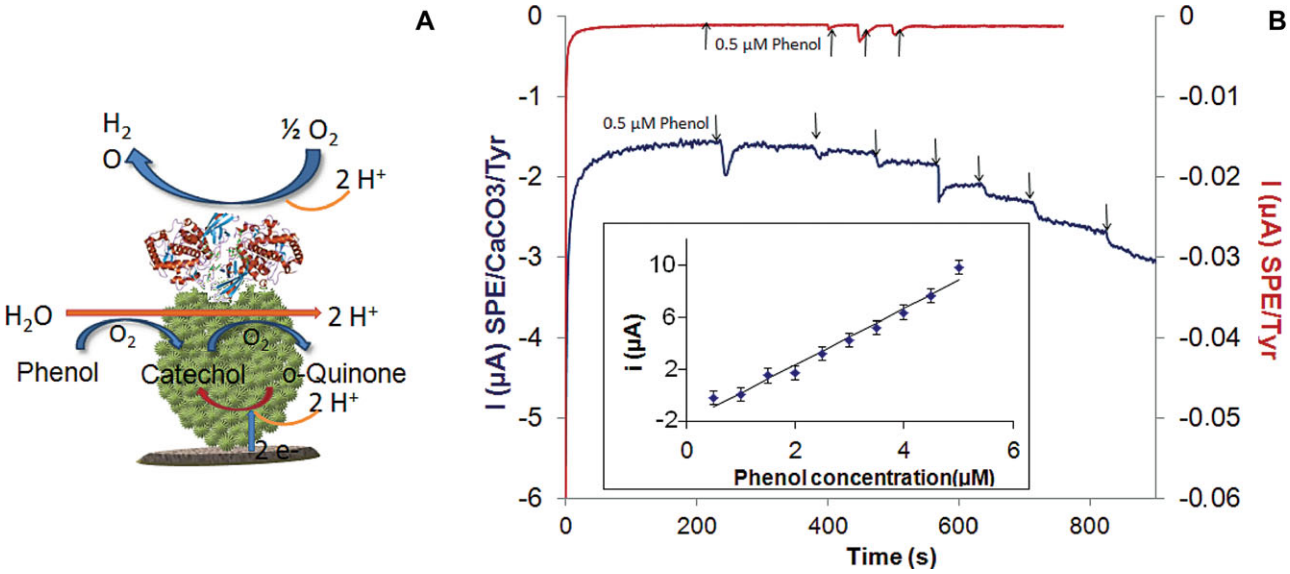

Figure 3. (A) Mechanism for the phenol bioelectrocatalytic detection using $CaCO_3$-PEI MPs. (B) Current–time response curves for the successive additions of 0.5 µM phenol standard solution in SPE/$CaCO_3$/tyrosinase (Tyr; blue line) and SPE/Tyr (red line). Inset: Biosensor calibration given as cathodic current versus phenol concentration. Working potential is –0.2 V. Other conditions as given in Section 2.

O-quinone (Eq. (2)). At moderately negative potential (−200 mV) the *O*-quinone product of phenol oxidation may be electrochemically reduced to catechol (Eq. (3)). Oxidation by the enzyme followed by reduction at the electrode may result in cycling between the catechol and *O*-quinone [5].

$$\text{Phenol} + H_2O \xrightarrow{Tyr(ox)\ /\ Tyr(red)} \text{Catechol} + 2H^+ + 2e^- \quad (1)$$

$$\text{Catechol} \xrightarrow{Tyr(ox)\ /\ Tyr(red)} \text{O-quinone} + 2H^+ + 2e^- \quad (2)$$

$$\text{O-quinone} + 2e^- + 2H^+ \xrightarrow{-200mV} \text{catechol} \quad (3)$$

The biosensors showed a rapid and sensitive bioelectrocatalytic response, reaching about 95% of the steady-state current within 40 s after each phenol-addition step. Inset of Fig. 3B shows the typical calibration curves of the SPE/$CaCO_3$-PEI/Tyr toward phenol. The obtained biosensing performance was as follows: linear response range from 0.5 to 5 µM with $r^2 = 0.9767$, LOD of 25 nM. LOD was calculated as the concentration corresponding to three times the SD of the estimate. The results of triplicate sets indicated by error bars reveal the repeatability (inset Fig. 3B) of the measurements with a RSD lower than 13%.

3.3 Implementation of the chronoamperometric detection in FIA chip microsystem

The study of the analytical performance of the developed PDMS/glass microchip was performed in FIA conditions by following the cathodic current and using the optimal conditions obtained: applied −0.2 V DC potential; pH 6.5; flow rate 500 µL/min; injection volume 20 µL. The typical current–time peaks were obtained for different phenol concentration injections using the PDMS/glass fluidic platform with integrated SPE modified with $CaCO_3$-PEI MPs and Tyr (see Fig. 4). Well-defined peaks were observed. The biosensor exhibited good response as a function of phenol concentration. In the phenol concentration range of 0.01–10 µM, phenol is characterized by a LOD of 5.1 nM, which is almost over five times lower than the level in batch measurements using the same system. LOD was calculated from the calibration equation as three times the *y*-intercept SD divided by the calibration slope. A RSD value for triplicate sets of 12.8% was obtained (Fig. 4B). The stability of this biosensor is related to the good entrapment of the enzyme within the $CaCO_3$-PEI and glutaraldehyde matrix indicating that plasma cleaner procedure used to bond PDMS and glass does not alter the activity of the biomembrane. On the other hand, the high biocatalytic activity of the SPE/$CaCO_3$-PEI/Tyr biosensor can be related with several factors. The enzyme is immobilized by adsorption onto the $CaCO_3$-PEI and remains entrapped onto the PEI surface via hydrogen bond between labile hydrogen in the biomolecule and PEI's nitrogen [9]. In addition an increase in the amount of active enzyme as a consequence of the enzyme activation by the presence of calcium may probably have occurred [17–20]. On the other hand, an improvement of the electron transfer through the $CaCO_3$-PEI composite is observed, all these phenomena contribute to

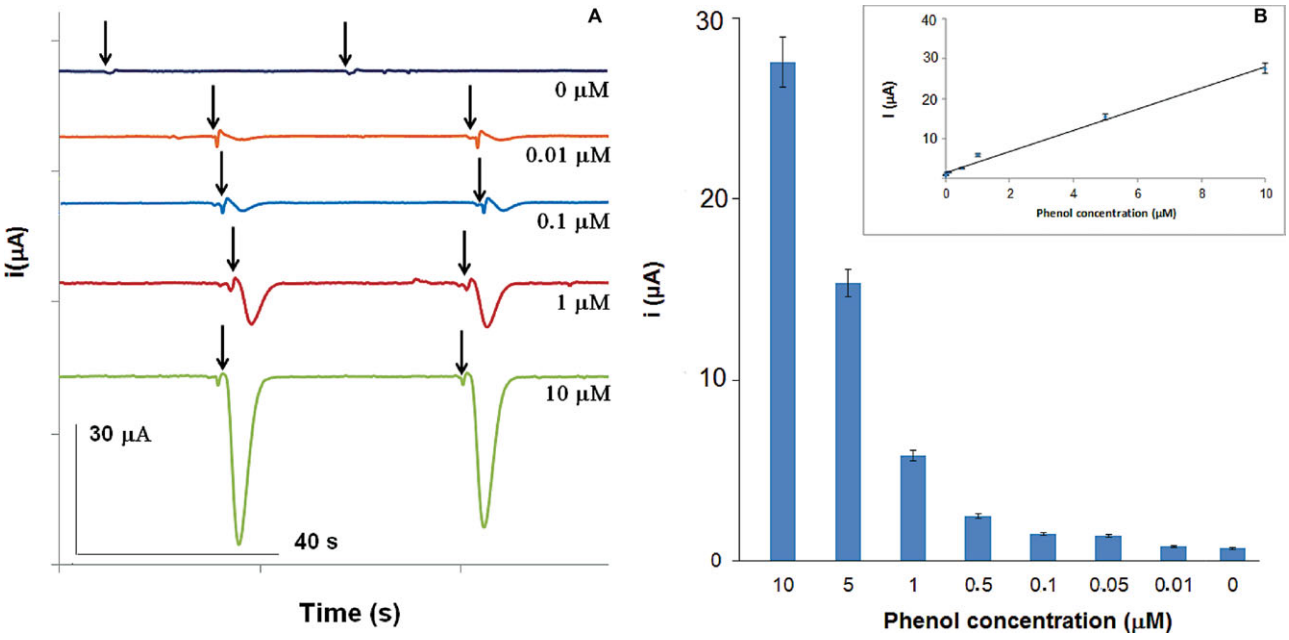

Figure 4. (A) Current–time responses for different phenol concentrations using fluidic microsystem. (B) Biosensor calibration curve given as cathodic current versus phenol concentration introduced in the PDMS/glass fluidic microsystem.

the high sensitivity and stability of this biosensor with interest in overall in situ and online monitoring applications (see Figs. 3B and 4).

The analytical performances of the proposed amperometric $CaCO_3$-PEI/Tyr based biosensor integrated to a flow microsystem were compared with other phenol biosensors integrated in microfluidic device reported in the literatures. The proposed FIA microsystem for phenol detection exhibited improved analytical performances in terms of a linear range and LOD in comparison with other microfluidic devices for phenol detection, such as phenol biosensor based on hydrogel microarrays entrapping Tyr and quantum dots [21], MCE with amperometric detection for a novel determination of phenolic compounds in olive oil [22], analytical microdevices for the detection of phenol using polymer hydrogel particles containing enzyme–quantum dot conjugates [23], and integrated microfluidics/electrochemical sensor system for monitoring of environmental exposures to lead and chlorophenols [7].

4 Concluding remarks

In this paper, a new system that allows the in situ and online phenol sensing using $CaCO_3$-PEI MPs in a PDMS/glass microchip was successfully implemented. This fluidic microsystem platform with the integrated $CaCO_3$-PEI/Tyr-based SPE is easy to be fabricated, inexpensive, disposable, and amenable to mass production. Very sensitive amperometric detection allowed phenol quantification at very low concentration (10 nM). The developed system uses a very low DC potential, decreasing this way the effect of inferences. On the other hand, the lower reagent consumption, inherent miniaturization, and versatility represent the main advantages of the developed device, which in the future could be used in automatic control systems with interest for environment monitoring between other applications.

This work is supported by the MICINN (Spain) grant for the Spain-Japan International Bilateral PIB2010JP-00278 project. A.L.M. thanks the Generalitat of Catalunya for the F12010 predoctoral scholarship given. L.H. and J.L. thank the support of the Scientific Grant Agency VEGA of the Slovak Republic (Project 1/0182/11).

The authors have declared no conflict of interest.

5 References

[1] Shan, D., Zhang, J., Xue, H.-G., Zhang, Y.-C., Cosnier, S., Ding, S. N., *Biosens. Bioelectron.* 2009, *24*, 3671–3676.

[2] Lu, L., Zhang, L., Zhang, X., Huan, S., Shen, G., Yu, R., *Anal. Chim. Acta* 2010, *665*, 146–151.

[3] Dimoglo, A., Akbulut, H. Y., Cihan, F., Karpuzcu, M., *Clean Techn. Environ. Policy* 2004, *6*, 288–295.

[4] Apetrei, C., Alessio, P., Constantino, C. J. L., de Saja, J. A., Rodriguez-Mendez, M. L., Pavinatto, F. J., Fernandes, E. G. R, Zucolotto, V., Oliveira, O. N., *Biosens. Bioelectron.* 2011, *26*, 2513–2519.

[5] Mayorga-Martinez, C. C., Cadevall, M., Guix, M., Ros, J., Merkoçi, A., *Biosens. Bioelectron.* 2012, *40*, 57–62.

[6] Popovtzer, R., Neufeld, T., Biran, D., Ron, E. Z., Rishpon, J., Shacham-Diamand, Y., *Nano Lett.* 2005, *5*, 1023–1027.

[7] Lin, Y., Timchalk, C. A., Matson, D. W., Wu, H., Thrall, K. D., *Biomed. Microdevices* 2001, *3*, 331–338.

[8] Star, A., Han, T.-R., Gabriel, J.-C. P., Bradley, K., Grüner, G., *Nano Lett.* 2003, *3*, 459–463.

[9] Lopez-Marzo, A., Pons, J., Merkoçi, A., *J. Mater. Chem.* 2012, *22*, 15326–15335.

[10] Solé, S., Merkoçi A., Alegret, S., *Anal. Chem.* 2003, *33*, 127–143.

[11] Medina-Sánchez, M., Miserere, S., Marín, S., Aragay, G., Merkoçi, A., *Lab. Chip.* 2012, *12*, 2000–2005.

[12] Pumera, M., Merkoçi, A., Alegret, S., *Trends Analyt. Chem.* 2006, *3*, 219–235.

[13] Devaraju, N. S. G. K., Unger, M. A., *Lab. Chip.* 2012, *12*, 4809–4815.

[14] Lalo, H. Ayela, C., Dague, E., Vieu, C., Haupt, K., *Lab. Chip.* 2010, *10*, 1316–1318.

[15] Mayorga-Martinez, C. C., Guix, M., Madrid, R. E., Merkoçi, A., *Chem. Commun.* 2012, *48*, 1686–1688.

[16] Alarcón, G., Guix, M., Ambrosi, A., Ramirez Silva, M. T., Palomar Pardave, M. E., Merkoçi, A., *Nanotechnology* 2010. *21*, 245502.

[17] Sanchez-Paniagua López, M., López-Cabarcos, E., López-Ruiz, B., *Sens. Actuators B: Chem.* 2012, *171–172*, 387–397.

[18] Sánchez-Paniagua López, M., Tamimi, F., López-Cabarcos, E., López-Ruiz, B., *Biosens. Bioelectron.* 2009, *24*, 2574–2579.

[19] Söderhäll, I., Bergenstråhle, A., Söderhäll, K., *Plant Physiol.* 1990, *93*, 657–661.

[20] Söderhäll, K., Carlberg, I., Eriksson, T., *Plant Physiol.* 1985, *78*, 730–733.

[21] Jang, E., Son, K. J., Kimb, B., Koh, W.-G., *Analyst* 2010, *135*, 2871–2878.

[22] Godoy-Caballero, M., Acedo-Valenzuela, M. I., Galeano-Díaz, T., Costa-García, A., Fernández-Abedul, M. T., *Analyst* 2012, *137*, 5153–5160.

[23] Park, S.-A. Jang, E., Koh, W.-G., Kim, B., *Talanta* 2011, *84*, 1000–1003.

